RSC Advances

PAPER

View Article Online
View Journal | View Issue

Cite this: *RSC Adv.*, 2017, **7**, 1101

A strategy for preparing spirobichroman dianhydride from bisphenol A and its resulting polyimide with low dielectric characteristic†

I Chun Tang,[a] Meng Wei Wang,[a] Chien Hsin Wu,[a] Shenghong A. Dai,*[b] Ru Jong Jeng*[a] and Ching Hsuan Lin*[b]

Received 22nd October 2016
Accepted 29th October 2016

DOI: 10.1039/c6ra25648a

www.rsc.org/advances

A spirobichroman dianhydride (**SBCDA**) was prepared through oxidation of an octamethyl spirobichroman (**OMSBC**), which was synthesized from acid-fragmentation of bisphenol A by 3,4-dimethylphenol, followed by Diels–Alder reaction. The reaction mechanism was proposed, and the optimal reaction conditions were discussed. Based on a high temperature solution polymerization of **SBCDA** and 4,4′-diaminodiphenylmethane (DDM), a spirobichroman-containing polyimide, **SBC-DDM**, was successfully prepared. Because of the contorted spiro-structure and rigid polymer backbone, **SBC-DDM** exhibits a large free volume, leading to outstanding organo-solubility and a low dielectric constant. In addition, the resulting film of **SBC-DDM** shows foldability, a high glass transition temperature, and good thermal stability.

Introduction

Because of the rigid main chain and strong intermolecular interactions, aromatic polyimides (PIs) exhibit many attractive properties, such as outstanding high-temperature stability,[1–3] good chemical and solvent resistance,[4] and excellent mechanical properties.[4,5] Based on their advantages, PIs have been applied in electronics,[6,7] optics, and membranes.[8,9] However, the rigid chain characteristics of PIs also lead to poor organo-solubility and high melting points, leading to limited processability. Thus, the processing of most commercial PIs was carried out with their precursors, poly(amic acid)s (PAAs), followed by thermal imidization. Unfortunately, it is difficult to store PAAs for a long period of time because of their thermal and hydrolytic instability.

To overcome the limitation of processability, increasing the free volume in PI matrix by introducing bulky groups, and non-coplanar structures into polymer chains has received much attention.[9–11] For example, Liou *et al.* introduced propeller-shaped triphenylamine (TPA) structures into polyimide backbones.[12,13] The non-coplanar TPA units effectively disrupt inter-chain packing, and the PIs were soluble in many aprotic solvents with good film-forming capability. In addition, the incorporation of spiroskeletons along the polymer backbones is also regarded as a successful approach to improve the organo-solubility without sacrificing much in thermal properties due to the non-coplanar and rigid characteristic of spiroskeletons.[14] Thomas *et al.* prepared an organo-soluble PI (soluble even in chloroform and dichloromethane) based on spirobifluorene diamine.[15] Hsiao *et al.* extended two kinds of spirobichroman diol **(1)–(2)** to spirobichroman dietheramines **(3)–(4)** and dietheranhydride **(5)**, respectively (Scheme 1).[16–18] Spirobichroman and diether-containing polyetherimides (PEIs) were further prepared, showing excellent organo-solubility.[16–18] However, the T_g values of these PEIs are in the range of 175–280 °C. Obviously, the diether linkages reduced the rigidity of polymer chains, leading to only moderate T_gs.

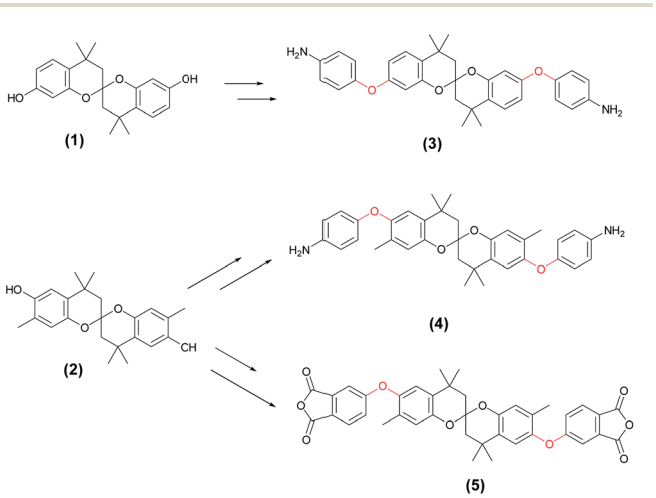

Scheme 1 Structure of **(1)–(5)**.

[a]*Institute of Polymer Science and Engineering, National Taiwan University, Taipei, Taiwan. E-mail: rujong@ntu.edu.tw*

[b]*Department of Chemical Engineering, National Chung Hsing University, Taichung, Taiwan. E-mail: shdai@dragon.nchu.edu.tw; linch@nchu.edu.tw*

† Electronic supplementary information (ESI) available. CCDC 1498507. For ESI and crystallographic data in CIF or other electronic format see DOI: 10.1039/c6ra25648a

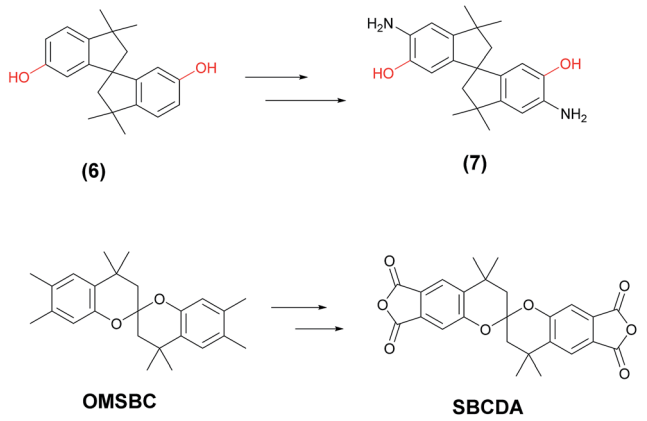

Scheme 2 Structure of (6)–(7), OMSBC, and SBCDA.

Generally, increasing the free volume in polymer matrix is also an effective approach for reducing dielectric constant. For example, Nagai *et al.* prepared 2,2′-bis(3,4-dicarboxyphenyl) hexafluoropropane dianhydride (6FDA)-based PIs to investigate the relationship of fractional free volume (FFV) and dielectric constant of PIs, concluding that the larger FFV of polymer brought about lower dielectric constant.[19] Zhang *et al.* prepared a (*E*)-N^1-(4-aminophenyl)-N^1-(4′-(2-phenyl-2-(4′-(trifluoromethyl)biphenyl-4-yl)vinyl)-biphenyl-4-yl)benzene-1,4-diamine-based polyimide, FPTTPI, containing a large nonplanar conjugated side chain.[20] In addition to the improvement of organo-solubility, the large free volume in FPTTPI film also led to excellent electrical properties, with a dielectric constant (D_k) of 1.52 at a frequency of 10 kHz.

On the concept of polymers of intrinsic microporosity (PIMs), contorted molecular structures combined with highly rigid polymer backbones can prevent the molecular packing efficiently, leading to larger free volume.[21] Pinnau and Han *et al.* reported that spiroskeleton-containing polyimides without the presence of flexible diether linkage could be prepared from a spiroindane diamine (**7**), which was synthesized by nitration of spiroindane bisphenol (**6**), followed by reduction (Scheme 2).[22] Apart from that, the resulting PIs exhibited large FFV (around 0.20), leading to excellent organo-solubility. However, the incorporation of polar hydroxyl groups enhanced the affinity of PIs to water. This would sacrifice the dielectric properties. For the purpose of obtaining a high-performance, organo-soluble, and low-dielectric polyimide, we provided a strategy for preparing a less polar spirobichroman dianhydride, **SBCDA**, for polyimide synthesis (Scheme 2).

The key for successfully synthesizing **SBCDA** is the derivatization from its precursor, octamethyl spirobichroman (**OMSBC**, Scheme 2). To the best of our knowledge, **OMSBC** has not been synthesized. However, the work done by Caruso *et al.*[23] gives us a light for **OMSBC** preparation. An acid-fragmentation of bisphenol A (BPA) by a exogenous phenol, such as *m*-cresol was attempted.[23] The phenol units of BPA were substituted by two exogenous phenols, and a tetramethyl xanthene derivative (see compound **2** in that work) with 72% yield was obtained (Scheme S1† lists the detailed mechanism for the transformation of compound **2**). According to gas chromatography-mass spectrometry (GCMS), a spiroketal compound (see compound **24** in that work) was observed in the initially formed product. Compound **24** afforded tetramethyl xanthene **2** when re-

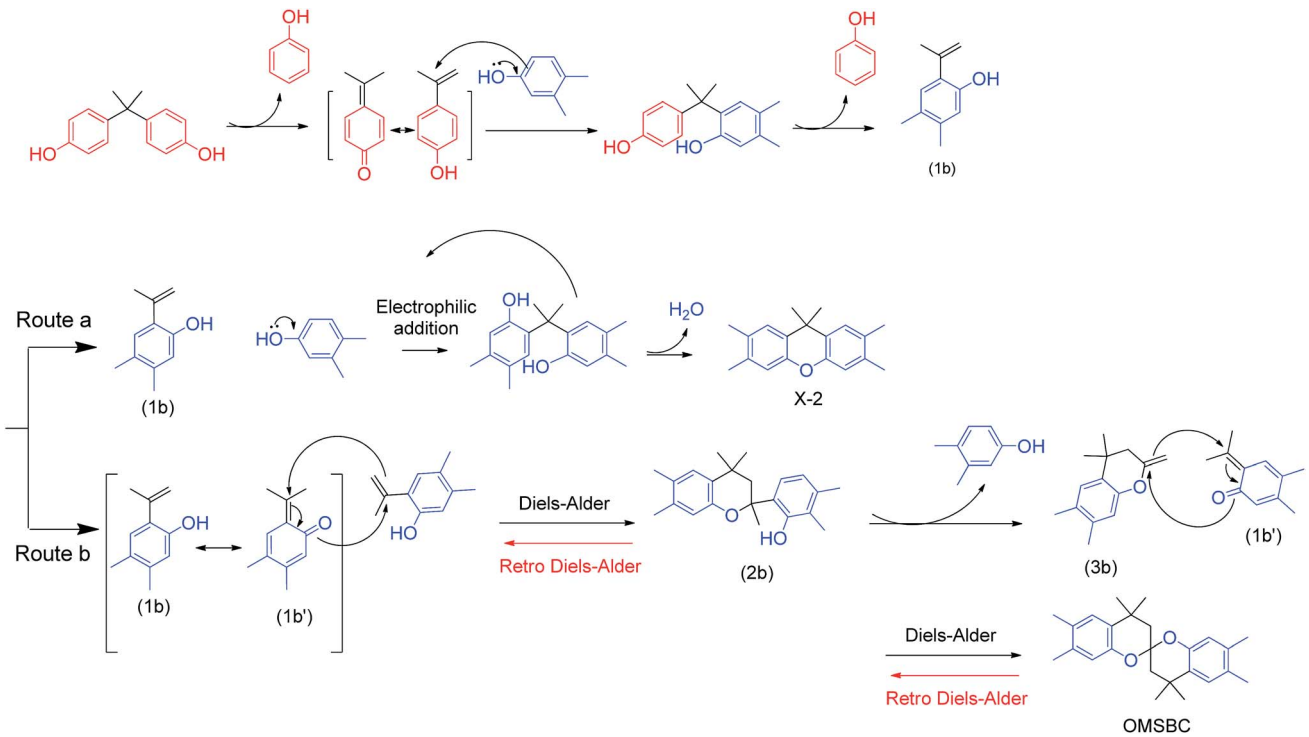

Scheme 3 Proposed synthetic route of **X-2** (Route a) and **OMSBC** (Route b).

subjected to the reaction conditions. Apparently, compound **24** is a kinetic product for the reaction. To explain the formation of compound **24**, a reaction mechanism including the acid fragmentation of BPA and twice Diels–Alder reactions was proposed.[20] However, the optimized reaction condition for compound **24** was not further elaborated. Moreover, spiro compound was not observed from the acid-fragmentation of BPA by 3,4-dimethylphenol. According to researches on Diels–Alder reaction,[24–26] retro Diels–Alder reaction will be occurred at high temperatures. Based on the above, we prepared **OMSBC** through acid-fragmentation of BPA by 3,4-dimethylphenol at low temperatures (Scheme 3). After oxidizing the tetramethyl of **OMSBC**, followed by condensation of diacid to dianhydride, the spirobichroman dianhydride, **SBCDA**, was obtained. Through a high temperature solution polymerization of **SBCDA** and 4,4′-diaminodiphenylmethane (DDM), a spirobichroman-containing polyimide, **SBC-DDM**, was successfully prepared. With the presence of spiroskeletons, rigid backbone, and hydrophobic aliphatic units (chroman and methylene groups), the polyimide, **SBC-DDM** exhibited outstanding organo-solubility and low dielectric constant. Detailed synthesis including optimal reaction conditions, characterizations, and properties were reported.

Experimental

Materials

Bisphenol A (BPA), manganese(II) acetate ($Mn(OAc)_2$), and cobalt(II) acetate ($Co(OAc)_2$) were purchased from Alfa. 3,4-Dimethylphenol and *t*-butyl cumyl peroxide (TBCP) were purchased from Acros. Sodium bromide (NaBr) and sodium hydroxide (NaOH) were purchased from Showa. Methane sulfonic acid (MSA) and isoquinoline were purchased from Fluka. 4,4′-Diaminodiphenylmethane (DDM) was purchased from Chriskev and recrystallized from methanol. Acetic acid glacial and *m*-cresol were purchased from Scharlau. All solvents are HPLC grade and were used without any further purification.

Characterization

NMR measurements were performed using a Varian Inova 400 NMR in DMSO-d_6 or $CDCl_3$. The chemical shift of ^{1}H NMR was calibrated by setting the chemical shift of trace amount of DMSO-d_5 in DMSO-d_6 as 2.49 ppm. Melting point measurements were performed by a Fargo Melting Point Apparatus MP-2D. Thermogravimetric analysis (TGA) was performed at a heating rate of 20 °C min^{-1} in flowing nitrogen or air (20 mL min^{-1}) by a Perkin-Elmer Pyris1. Thermomechanical analysis (TMA) was performed with a sample size of 10 mm × 5 mm using a SII TMA/SS6100. The analysis was performed at a heating rate of 5 °C min^{-1} from 40 to 350 °C without N_2 or air flow. The coefficient of thermal expansion (CTE) was recorded from the second-run in three kinds of temperature ranges. IR spectra were obtained from at least 32 scans in the standard wavenumber range of 650–4000 cm^{-1} using a PerkinElmer RX1 infrared spectrophotometer. Gel permeation chromatography (GPC) was carried out on a Hitachi LaChrom Elite using *N*-methyl-2-pyrrolidone (NMP) as the eluent at 60 °C with a flow rate of 0.6 mL min^{-1}. The molecular weights were calibrated with polystyrene standard. Elemental analysis was performed on an Elementar Vario EL III (CHN-OS Rapid, German). The accuracy and precision of this instrument are 0.1% and 0.2%, respectively. Acetanilide and benzoic acid were used as standards and the data of them as follows: N 10.36%, C 71.09%, H 6.71% for acetanilide; O 26.20% for benzoic acid. The X-ray crystallographic data were collected on a Bruker D8 VENTURE. High resolution mass (HRMS) measurements were performed by a Finnigan/Thermo Quest MAT 95XL mass spectrometer by electron impact ionization. The dielectric constant of the polymer film was measured without any preprocess at a frequency of 100 MHz and 1 GHz, using Agilent E4991A RF impedance/material analyzer with a sample size of 1 cm × 1 cm × 150 μm. Experimental data was obtained from at least 5 times for each test.

Synthesis of octamethyl spirobichroman (OMSBC)

BPA 20.60 g (0.09 mol) and 3,4-dimethylphenol 77.14 g (0.63 mol) were introduced into a 500 mL round-bottom glass flask equipped with a nitrogen inlet, and a magnetic stirrer. The reaction mixture was stirred continuously at 80 °C until the reagents melted completely. MSA 4.12 g (20 wt% based on BPA) was then added to the reaction mixture, which was further stirred at 80 °C for 4 h. Subsequently, the reaction temperature was cooled to room temperature. The mixture was dissolved in toluene, washed with 10 wt% NaOH solution, and rinsed with water. Toluene was removed using a rotary evaporator and then the crude product was washed with hot methanol to remove xanthene derivatives (will be discussed in 3.1). The purified product was collected by filtration and dried in vacuum at 60 °C. White powders (20% yield) were obtained with a melting point of 180 °C. HR-MS (EI) *m*/*z*: calcd for $C_{25}H_{32}O_2$ 364.2402; anal., for 364.2393. Elem. anal. calcd C, 82.37%; H, 8.85%; O, 8.78%. Found: C, 82.60%; H, 9.05%; O, 8.32%. ^{1}H-NMR (DMSO-d_6), δ = 7.1 ppm (s, 2H, H_4), 6.3 ppm (s, 2H, H_7), 2.1 ppm (s, 6H, H_5), 2.0 ppm (s, 6H, H_6), 1.8–2.1 ppm (d–d, 4H, H_1), 1.5 ppm (s, 6H, H_3), 1.2 ppm (s, 6H, H_2).

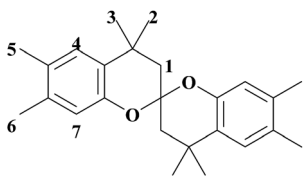

Synthesis of spirobichroman dianhydride (SBCDA)

To a Parr reactor equipped with a oxygen inlet, **OMSBC** 5.00 g (0.014 mol), $Mn(OAc)_2$ 0.10 g, $Co(OAc)_2$ 0.10 g, NaBr 0.10 g, TBCP 0.20 g, and acetic anhydride 40 mL were added. After the reaction system was purged with oxygen eight times, the pressure of the Parr reactor was kept at 250–300 psi under oxygen atmosphere. The reaction mixture was stirred at 170–180 °C for 11 h. After the reaction was complete and the reactor was cooled to room temperature, the solution was filtered. The filtrate was

poured into 500 mL water and filtered again. The raw product was refluxed in acetic anhydride for 5 h. After cooling to room temperature, the crystalline product was filtered and dried in vacuum at 80 °C. Yellow green crystals (11% yield) were obtained. HR-MS (EI) *m*/*z*: calcd for $C_{25}H_{20}O_8$ 448.1158; anal., for 448.1154. Elem. anal. calcd C, 66.96%; H, 4.50%; O, 28.54%. Found: C, 65.01%; H, 4.38%; O, 29.30%. ^{1}H-NMR (DMSO-d_6), δ = 8.3 ppm (s, 2H, H_4), 7.3 ppm (s, 2H, H_5), 2.2–2.4 ppm (d–d, 4H, H_1), 1.7 ppm (s, 6H, H_3), 1.4 ppm (s, 6H, H_2). FTIR (KBr): 1839 and 1770 cm^{-1} (C=O stretch).

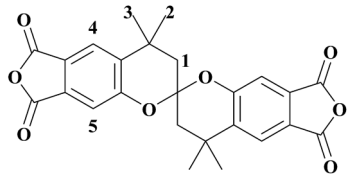

Preparation of SBC-DDM

DDM 0.4342 g (2.19 mmol) and *m*-cresol 8.02 g were introduced into a 100 mL round-bottom glass flask equipped with a nitrogen inlet, and a magnetic stirrer. After the diamine was dissolved completely, **SBCDA** 0.9821 g (2.19 mmol) and 2 drops of isoquinoline were added. The mixture was reacted at 170 °C for 12 h. Subsequently, the viscous solution was poured into methanol giving rise to a brown fibrous precipitate (90% yield) that was collected by filtration, and dried in vacuum at 70 °C. ^{1}H-NMR ($CDCl_3$), δ = 8.0 ppm (s, 2H, H_5), 7.3 ppm (d, 8H, H_6 and H_7), 7.1 ppm (s, 2H, H_1), 4.1 ppm (s, 2H, H_8), 2.2 ppm (d–d, 4H, H_4), 1.8 ppm (s, 6H, H_2), 1.4 ppm (s, 6H, H_3).

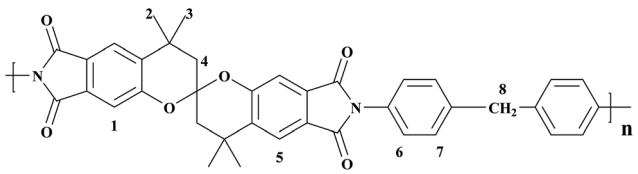

Preparation of the polyimide film

A solution of the polymer was prepared by dissolving 0.4 g of **SBC-DDM** in 2 mL of NMP. The homogeneous solution was cast onto a glass substrate and heated in an oven at 80 °C for 12 h to remove most of the solvent; then the semi-dried film was further dried in vacuum at 100 °C (1 h), followed by 200 °C (1 h). An automatic film applicator BRAIVE/B-4300 was used for coating procedure. The solution was cast on glass by setting a controlling gap thickness of 200 μm. The resulting thin film was around 10 μm thick and sectioned to controlled geometries for TMA and dielectric measurement.

Results and discussion

Synthesis of OMSBC

To prepare **OMSBC**, the acid-fragmentation of BPA by 3,4-dimethylphenol was performed at various reaction conditions (Table 1).

Firstly, we followed Caruso's work,[23] using 100 °C as reaction temperature. But a xanthene derivative, **X-2** (the structure was shown in Scheme 3), was the only product (Run 1). The assignment in ^{1}H NMR spectrum (Fig. S1, ESI†) supports the structure of **X-2**. Based on the mechanism reported by Caruso *et al.*,[23] we proposed a possible mechanism as shown in Scheme 3. Initially, the acid fragmentation of BPA by 3,4-dimethylphenol leads to 2-isopropenylene-4,5-dimethylphenol (**1b**). Two possible routes for further reactions of (**1b**) were proposed. Route a explains the formation of **X-2**, while Route b explains the formation of **OMSBC**. In Route a, an electrophilic substitution between 3,4-dimethylphenol and (**1b**) occurred, leading to the formation of **X-2**. On the concept of this mechanism, we reduced the amount of 3,4-dimethylphenol to decrease the probability of electrophilic addition between (**1b**) and 3,4-dimethylphenol, avoiding the formation of **X-2**. However, the results of both entries are the same as that of Run 1 (only xanthene **X-2** was obtained in Run 2–3). Changing the ratio of BPA/3,4-dimethylphenol has no effect on the outcome of products. Furthermore, we reduced reaction temperature to 80 °C, leading to a mixture of **OMSBC** and **X-2**. The result agrees with our speculation that a high temperature reaction conditions favors **X-2**, while low temperature reaction condition leads to the formation of **OMSBC**. The yield of **OMSBC** was improved by reducing the amount of 3,4-dimethylphenol added to the reaction. However, the yield was decreased when much less amount of 3,4-dimethylphenol was added to the reaction. Therefore, a highest isolated yield occurred in Run 6 was established. We suggest that the formation of the key intermediate (**1b**) became more difficult in Run 7, leading to the reduced yield of **OMSBC**. The ^{1}H-NMR spectrum of **OMSBC** was shown in Fig. 1(a), and the assignment supports its structure. In Route b, a Diels–Alder reaction between (**1b**) and its tautomer (**1b′**) leads to (**2b**). Then, a presumed chroman (**3b**) would be generated by leaving one 3,4-dimethylphenol. Chroman (**3b**) acts as a dienophile for the second Diels–Alder reaction with (**1b′**), leading to the formation of **OMSBC**. Since high temperatures favor retro Diels–Alder reaction, Route b is not a preferred route at high temperatures.

This mechanism explains the result in Table 1 that reacting at above 100 °C leads to only **X-2**, while reacting at 80 °C leads to mixture of **X-2** and **OMSBC**. However, an attempt to enhance the yield of **OMSBC** *via* further reducing the reaction temperature to 60 °C was failed due to the fact that the melting point of 3,4-dimethylphenol was 68 °C.

To discuss the influence of reaction time, we used the best reaction condition in Table 1 (Run 6) to perform ^{1}H NMR trace at various stages of reaction. Fig. S2 (ESI†) shows ^{1}H NMR trace for **OMSBC** synthesis after 24 h and 48 h of reaction, respectively. The benzene signals of **OMSBC** at 7.1 and 6.3 ppm decreased; on the other hand, the benzene signals of **X-2** at 7.2 and 6.8 ppm increased with increasing reaction time. This implies that retro Diels–Alder reaction still occurred in the presence of acid catalyst at low temperatures (80 °C), leading to the transformation of **OMSBC** to **X-2**. Scheme S2† shows the proposed mechanism on retro Diels–Alder reaction of **OMSBC** in the presence of methanesulfonic acid (MsOH). The first retro

Table 1 Reaction conditions for the synthesis of OMSBC

Run[a]	Molar ratio (BPA/ 3,4-dimethylphenol)	Temperature (°C)	Product	Isolated **OMSBC** yield (%)
1	1/20	100	**X-2**	0
2	1/10	100	**X-2**	0
3	1/5	100	**X-2**	0
4	1/20	80	**X-2** + **OMSBC**	3
5	1/10	80	**X-2** + **OMSBC**	10
6	1/7	80	**X-2** + **OMSBC**	14
7	1/5	80	**X-2** + **OMSBC**	10

[a] Reaction time is 24 h; the acid catalyst is methanesulfonic acid (20 wt% based on BPA).

Diels–Alder reaction was initiated by protonation on the oxygen of **OMSBC** and releasing of (**1b′**), leading to the formation of intermediate (**3b**). Subsequently, the intermediate (**2b**) was generated by acid-catalyzed electrophilic addition of (**3b**) with 3,4-dimethylphenol. After protonation on the oxygen of (**2b**), the second retro Diels–Alder reaction was carried out, leading to the formation of (**1b**) and its tautomer (**1b′**).

To avoid the retro Diels–Alder reaction, we shortened the reaction time and further monitored the reaction by ^{1}H NMR trace (Fig. S3†). The benzene signals of **OMSBC** at 7.1 and 6.3 ppm were observed after 1 h, and reached a maximum after 4 h. After that, the benzene signals slightly decreased, and the impurity signals (around 6–7 ppm in Fig. S3†) increased with increasing reaction time, demonstrating that the retro Diels–Alder reaction occurred after 5 h. After optimizing the reaction conditions, a maximum yield around 20% of synthesizing **OMSBC** was achieved in this work.

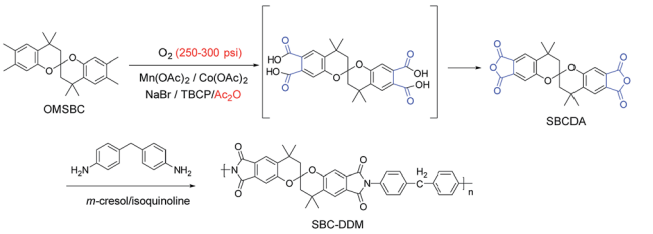

Scheme 4 Synthesis of SBCDA and its derived polyimide SBC-DDM.

Synthesis of SBCDA

As shown in Scheme 4, a spirobichroman dianhydride (**SBCDA**) was prepared by the oxidation of the *ortho*-dimethyl groups of **OMSBC**, followed by chemical cyclodehydration with acetic anhydride. As mentioned earlier, retro Diels–Alder reaction of **OMSBC** would occur in the presence of acid catalyst (Scheme S2†). Therefore, acetic anhydride was used as solvent for the oxidation procedure instead of acetic acid.[27,28] Experimental data show that the methyl groups of **OMSBC** were transferred to carboxylic acids incompletely under standard pressure. Fig. 1(b) shows ^{1}H NMR spectrum of **SBCDA**. As compared with the spectrum of **OMSBC**, the characteristic peaks of benzene shifted from 7.1 to 8.3 ppm and 6.3 to 7.3 ppm. The chemical shifts are more downfield due to the formation of carbonyl groups, which exhibit strong electron-withdrawing characteristic. In addition, the characteristic peaks of methyl group on benzene disappeared in Fig. 1(b), confirming the structure of **SBCDA**. Fig. 2 shows FTIR spectra of **OMSBC** and **SBCDA**. The characteristic absorptions at 1839 (C=O asymmetric stretch) and 1770 cm^{-1} (C=O symmetric stretch) further confirm the structure of **SBCDA**.

The structural configuration of **SBCDA** was confirmed by single crystal diffractogram, as shown in Fig. 3. The detailed diffraction data of **SBCDA** is listed in Tables S1–S5 (ESI†). As seen in Fig. 3, the non-coplanar **SBCDA** compound provides

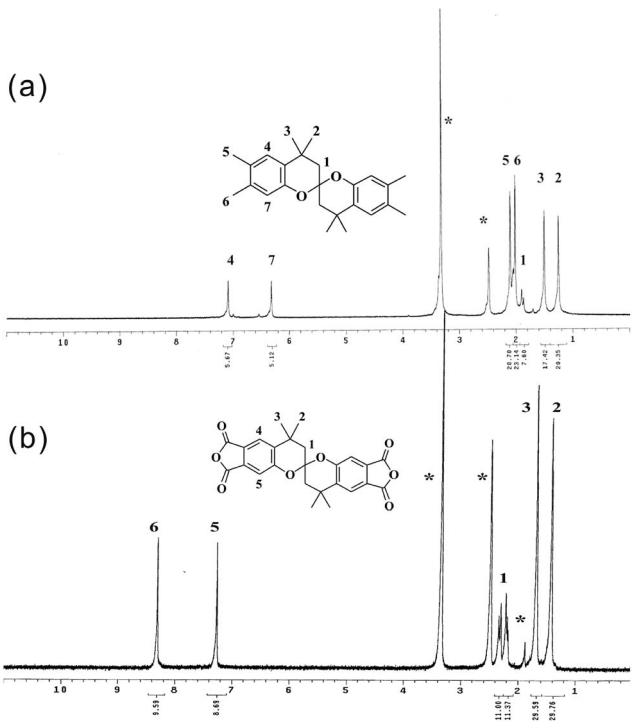

Fig. 1 ^{1}H NMR spectrum of (a) **OMSBC** and (b) **SBCDA**.

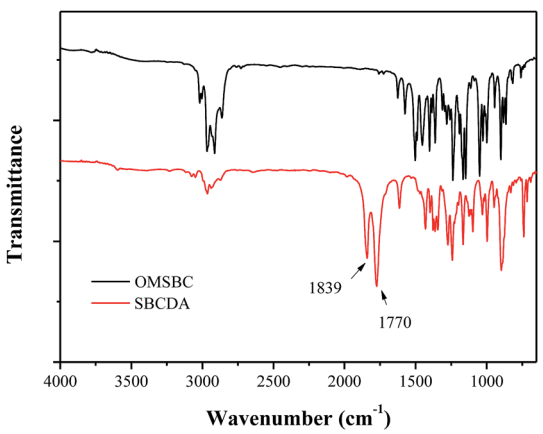

Fig. 2 FTIR spectra of **OMSBC** and **SBCDA**.

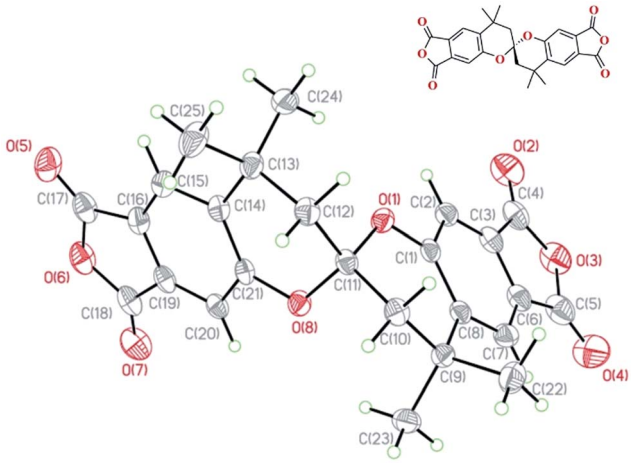

Fig. 3 Single crystal diffractogram of **SBCDA**.

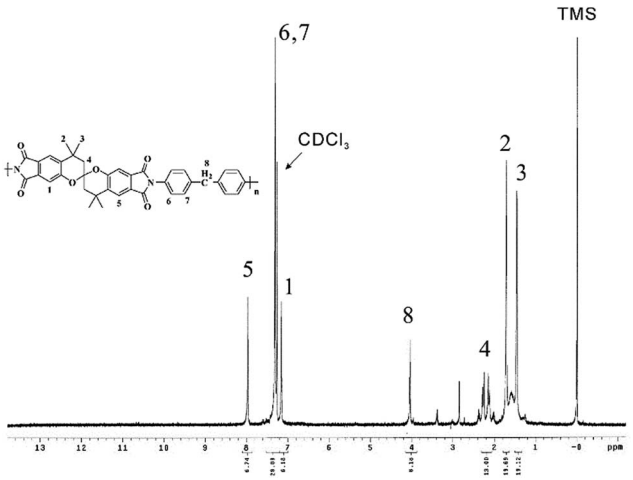

Fig. 4 ^{1}H NMR spectrum of **SBC-DDM** in $CDCl_3$.

a site of contortion due to the presence of spirobichroman unit, demonstrating that the molecular packing of its derived polymers can be restricted.[21,22] The spectroscopic data in Fig. 1–3 support the synthesis of **SBCDA** through the high-temperature (170–180 °C) and high-pressure (250–300 psi) procedure.

Polyimide synthesis

SBC-DDM was prepared by the one-pot, high temperature solution polymerization of **SBCDA** with 4,4′-diaminodiphenylmethane (DDM) in *m*-cresol in the presence of isoquinoline (Scheme 4). After reaction was completed, the polymer solution became highly viscous and fiber-like product could be precipitated in methanol. Due to the outstanding organo-solubility (to be discussed later), **SBC-DDM** can be dissolved in $CDCl_3$ for ^{1}H NMR spectroscopic analysis (Fig. 4). The assignment of each peak is detailed in the figure, confirming the structure of **SBC-DDM**. GPC data of **SBC-DDM** was measured using *N*-methyl-2-pyrrolidinone (NMP) as eluent. The number-average molecular weight (M_n) and weight-average molecular weight (M_w) are 7.0×10^4 and 17.2×10^4 g mol^{-1}, respectively. Fig. 5 shows the photos of **SBC-DDM** film *via* solution casting. As seen in the figure, the transparent and foldable film further supports the high molecular weight of **SBC-DDM**.

Physical and electric properties

The fractional free volume (FFV) was calculated by using the following relationship:[29–31]

$$V = M/\rho \quad (1)$$

$$\mathrm{FFV} = \frac{(V - 1.3V_w)}{V} \quad (2)$$

where V is the molar volume (cm^3 mol^{-1}) of the polymer, M is the molar mass (g mol^{-1}) of the polymer, and ρ is the density (g cm^{-3}) of the polymer, which was measured experimentally (determined by measurements of the weight in air and in deionized water). V_w is the van der Waals volume (cm^3 mol^{-1}) of polymer. According to literature,[29–31] V_w is often calculated from Bondi's group contribution method.[32–34] However, it is very time-consuming and easy to make a miscalculation for complex compounds. To simplify the calculation of V_w, a fast method has been reported by Abraham.[35] Eqn (3) based on Bondi radii was used to calculate V_w in this work:

$$V_{vdw}\ (\text{Å}^3 \text{ per molecule}) = \Sigma_{\text{all atom contributions}} - 5.92N_B - 14.7R_A - 3.8R_{NA} \quad (3)$$

$$N_B = N - 1 + R_g \quad (4)$$

$$R_g = R_A + R_{NA} \quad (5)$$

where N is the total number of atoms, R_A and R_{NA} are the number of aromatic and nonaromatic rings, respectively. All atomic volume contributions are referred to literature[35] (see Table 2 of this literature). Herein, we converted the unit from Å^3 per molecule to cm^3 mol^{-1} by multiplying by 0.602. The results are listed in Table 2. To investigate the relationship of free volume and chemical structure, a commercial polyimide, **PMDA-ODA**, was used for comparison. The FFV of **SBC-DDM** (0.20) is higher than that of **PMDA-ODA** (0.05), demonstrating that the molecular packing can be disrupted effectively by

Fig. 5 Photo of **SBC-DDM** film.

Table 2 Physical properties of SBC-DDM

Sample ID	ρ (g cm^{-3})	V (cm^3 mol^{-1})	M (g mol^{-1})	V_w (cm^3 mol^{-1})	FFV
SBC-DDM	1.13	538.98	610.67	333.1	0.20
PMDA–ODA[a]	1.39	275.0	382.3	194.8	0.05
PIM-PMDA–OH[b]	1.18	NA[c]	NA	NA	0.20
PIM-6FDA–OH[b]	1.22	NA	NA	NA	0.23

[a] Prepared from pyromellitic dianhydride (PMDA) and 4,4′-diaminodiphenylether (ODA). [b] Data from ref. 22. [c] Not available.

introducing a spirobichroman into polymer backbone. Further comparison with spiroindane-containing polyimides which prepared by Han *et al.*,[22] the FFV of **SBC-DDM** is the same as that of PIM-PMDA–OH (0.20), supporting that the introduction of spirobichroman unit into rigid polymer backbones would enhance the FFV of polymer. However, the FFV of **SBC-DDM** is slightly lower than that of PIM-6FDA–OH (0.23) due to the absence of bulky trifluoromethyl ($-CF_3$) groups.

The solubility properties of **SBC-DDM** are listed in Table 3. Owing to the large FFV, **SBC-DDM** exhibited outstanding organo-solubility. Different from many organo-soluble polyimides, **SBC-DDM** can be more easily dissolved in borderline polar and nonpolar aprotic solvents such as THF, $CHCl_3$ and CH_2Cl_2 than in polar aprotic solvents (such as DMF and DMSO). This is due to the incorporation of hydrophobic chroman and methylene units in **SBC-DDM**. When compared with the diether and spirobichroman-containing polyetherimide **7f** (the structure is shown in Table 3),[16] diether-free **SBC-DDM** exhibits superior organo-solubility (Table 3).

To study the influence of conformational changes in polymers, molecular modeling analysis of **SBC-DDM** with two spirobichroman units were performed by using ChemBio3D Ultra software as shown in Fig. 6. It is postulated that the rigid backbone combined with the contorted spiro-structure in **SBC-DDM** prevent an efficient packing and entanglement in polymer chain, contributing to the organo-solubility.

The dielectric constant of **SBC-DDM** was 2.451 ± 0.001 and 2.342 ± 0.001 at a frequency of 100 MHz and 1 GHz, respectively. Owing to the large FFV and hydrophobic aliphatic structures, **SBC-DDM** exhibited much lower dielectric constant than did PMDA–ODA (around 3.1–3.5),[36] showing the low dielectric characteristic. As a result, the introduction of spiroskeleons into rigid polymer backbone is beneficial to increase the free volume in polymer matrix, improve the organo-solubility and reduce dielectric constant.

Table 3 Solubility properties of SBC-DDM and referenced PEI **7f**[16]

	Solvent[a]						
Sample ID	NMP	DMF	DMSO	*m*-Cresol	CH_2Cl_2	$CHCl_3$	THF
SBC-DDM	+[b]	+h	+h	+	+	+	+
7f[d]	+	+	−	+	NA[c]	+	+

[a] Solubility was tested with a 5 mg sample in 0.5 mL of solvent. [b] +, soluble at room temperature; +h, soluble on heating; −, insoluble on heating. [c] Not available. [d] Structure of **7f**:

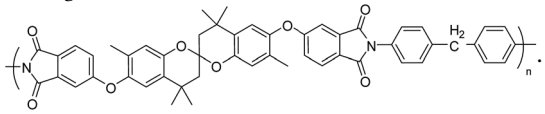

Thermal properties

Fig. 7(a) shows the TMA thermogram of **SBC-DDM**. The T_g value, defined by on onset temperature of the TMA thermogram, is 343 °C. On the other hand, the T_g value of the referenced PEI **7f** is 235 °C,[16] demonstrating that the higher rigidity of diether-free **SBC-DDM** contributes to the improved thermal properties. The coefficient of thermal expansion (CTE) of **SBC-DDM** in the temperature range of 50–150 °C is around 41 ppm °C^{-1}, suggesting a remarkable dimensional stability at low temperature. However, the CTE decreased to a negative value (−130 ppm °C^{-1}) in the temperature range of 200–300 °C. According to Hasegawa's report,[37] we suggested that the high rigidity backbone and contorted spiro-structure in **SBC-DDM** contributes to a high level of in-plane orientation of PI main chains and a decrease in crystallinity, leading to thermal contraction in **SBC-DDM**. Furthermore, the CTE value increased rapidly with further increasing temperature due to the softening of the polyimide film under the tension mode. The 10 wt%

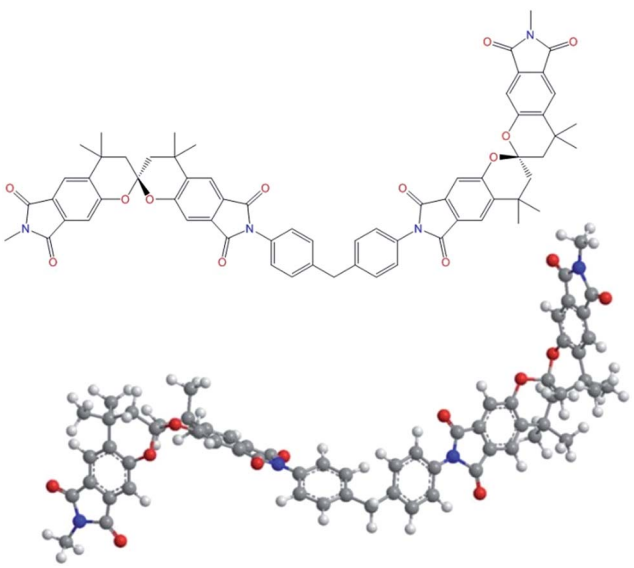

Fig. 6 Molecular models of SBC-DDM as calculated with energy minimization.

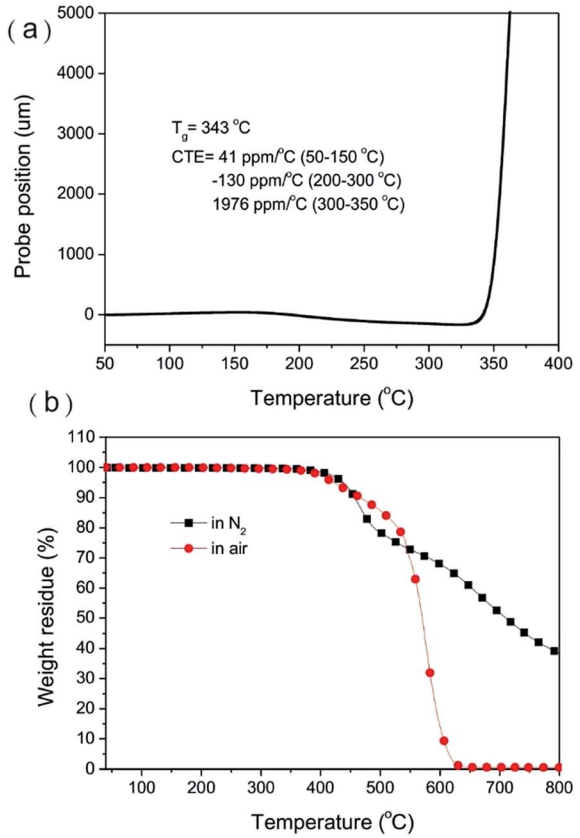

Fig. 7 (a) TMA and (b) TGA thermogram of **SBC-DDM**.

decomposition temperature (T_{d10}) in air atmosphere (467 °C) is higher than in a nitrogen atmosphere (457 °C) because of the oxidation of aliphatic segments as reported in literature.[16] As compared with the T_{d10} of referenced PEI **7f** (457 and 454 °C in air and N_2, respectively),[16] **SBC-DDM** exhibits somewhat better thermal stability due to the absence of diether linkage. In addition, the char yield of **SBC-DDM** at 800 °C in a nitrogen atmosphere is around 38%, which is similar to that of **7f** (41%).[16] Indeed, **SBC-DDM** exhibits good thermal stability, suggesting that the spirobichroman unit is stable at high temperatures without the presence of acid catalyst.

Conclusions

We have successfully synthesized an octamethyl spirobichroman (**OMSBC**) through the acid-fragmentation of BPA by 3,4-dimethylphenol. The synthesis is sensitive to the reaction temperatures. A reaction mechanism was proposed in Scheme 1 to explain the fact that reacting at above 100 °C leads to only **X-2**, while reacting at 80 °C leads to mixture of **X-2** and **OMSBC**. Through high pressure oxidation of **OMSBC** at high temperatures, a spirobichroman dianhydride (**SBCDA**) was newly developed. **SBCDA** was used to prepare a high performance polyimide (**SBC-DDM**) by a high temperature solution polymerization with **DDM**. After solution casting, a transparent and foldable film was obtained. Due to the contorted spirobichroman units leading to large free volume (Table 2), the polyimide, **SBC-DDM** possessed outstanding organo-solubility (Table 3) and a low-dielectric constant (2.34 at 1 GHz). **SBC-DDM** exhibits much higher thermal properties (Fig. 7) than did a spirobichroman diethertanhydride-based polyetherimide (**7f** in Hsiao's work[16]). The combination of organosolubility, high-T_g and low-dielectric properties make **SBC-DDM** attractive for electronic applications.

Acknowledgements

Financial support on this work from the Ministry of Science and Technology, Taiwan is highly appreciated.

References

1 J. P. Gao and Z. Y. Wang, *J. Polym. Sci., Part A: Polym. Chem.*, 1995, **33**, 1627–1635.
2 A. Kausar, S. Zulfiqar, Z. Ahmad and M. I. Sarwar, *Polym. Degrad. Stab.*, 2010, **95**, 1826–1833.
3 H.-L. Lin, T.-Y. Juang, L.-H. Chan, R.-H. Lee, S. A. Dai, Y.-L. Liu, W.-C. Su and R.-J. Jeng, *Polym. Chem.*, 2011, **2**, 685–693.
4 M. G. Dhara and S. Banerjee, *Prog. Polym. Sci.*, 2010, **35**, 1022–1077.
5 D. M. Stoakley, A. K. S. Clair and C. I. Croall, *J. Appl. Polym. Sci.*, 1994, **51**, 1479–1483.
6 O. J. Dautel, G. Wantz, D. Flot, J.-P. Lere-Porte, J. J. E. Moreau, J.-P. Parneix, F. Serein-Spirau and L. Vignau, *J. Mater. Chem.*, 2005, **15**, 4446–4452.
7 X. Jia, D. Chao, H. Liu, L. He, T. Zheng, X. Bian and C. Wang, *Polym. Chem.*, 2011, **2**, 1300–1306.
8 Y. Xiao, B. T. Low, S. S. Hosseini, T. S. Chung and D. R. Paul, *Prog. Polym. Sci.*, 2009, **34**, 561–580.
9 H.-J. Yen and G.-S. Liou, *Polym. Chem.*, 2012, **3**, 255–264.
10 A. Ghosh, S. K. Sen, S. Banerjee and B. Voit, *RSC Adv.*, 2012, **2**, 5900–5926.
11 X. Ma, O. Salinas, E. Litwiller and I. Pinnau, *Polym. Chem.*, 2014, **5**, 6914–6922.
12 H.-J. Yen, J.-H. Wu, Y.-H. Huang, W.-C. Wang, K.-R. Lee and G.-S. Liou, *Polym. Chem.*, 2014, **5**, 4219–4226.
13 C.-W. Chang, H.-J. Yen, K.-Y. Huang, J.-M. Yeh and G.-S. Liou, *J. Polym. Sci., Part A: Polym. Chem.*, 2008, **46**, 7937–7949.
14 S. Zhang, Y. Li, T. Ma, J. Zhao, X. Xu, F. Yang and X.-Y. Xiang, *Polym. Chem.*, 2010, **1**, 485–493.
15 J. Weber, Q. Su, M. Antonietti and A. Thomas, *Macromol. Rapid Commun.*, 2007, **28**, 1871–1876.
16 S.-H. Hsiao and C.-Y. Yang, *J. Polym. Sci., Part A: Polym. Chem.*, 1997, **35**, 2801–2809.
17 S.-H. Hsiao, C.-P. Yang and C.-Y. Yang, *J. Polym. Sci., Part A: Polym. Chem.*, 1997, **35**, 1487–1497.
18 S.-H. Hsiao and C.-Y. Yang, *Macromol. Chem. Phys.*, 1997, **198**, 2181–2195.
19 S. Miyata, S. Sato, K. Nagai, T. Nakagawa and K. Kudo, *J. Appl. Polym. Sci.*, 2008, **107**, 3933–3944.

20 Y. Liu, C. Qian, L. Qu, Y. Wu, Y. Zhang, X. Wu, B. Zou, W. Chen, Z. Chen, Z. Chi, S. Liu, X. Chen and J. Xu, *Chem. Mater.*, 2015, **27**, 6543–6549.
21 P. M. Budd, B. S. Ghanem, S. Makhseed, N. B. McKeown, K. J. Msayib and C. E. Tattershall, *Chem. Commun.*, 2004, 230–231.
22 X. Ma, R. Swaidan, Y. Belmabkhout, Y. Zhu, E. Litwiller, M. Jouiad, I. Pinnau and Y. Han, *Macromolecules*, 2012, **45**, 3841–3849.
23 A. J. Caruso and J. L. Lee, *J. Org. Chem.*, 1997, **62**, 1058–1063.
24 N. Kuramoto, K. Hayashi and K. Nagai, *J. Polym. Sci., Part A: Polym. Chem.*, 1994, **32**, 2501–2504.
25 Y.-L. Liu, C.-Y. Hsieh and Y.-W. Chen, *Polymer*, 2006, **47**, 2581–2586.
26 E. Goiti, M. B. Huglin and J. M. Rego, *Macromol. Rapid Commun.*, 2003, **24**, 692–696.
27 C. H. Lin, C. M. Huang, M. W. Wang, S. A. Dai, H. C. Chang and T. Y. Juang, *J. Polym. Sci., Part A: Polym. Chem.*, 2014, **52**, 424–434.
28 M.-C. Kuo, Y.-C. Tung, C.-L. Yeh, H.-Y. Chang, R.-J. Jeng and S. A. Dai, *Macromolecules*, 2008, **41**, 9637–9642.
29 N. Du, G. P. Robertson, I. Pinnau and M. D. Guiver, *Macromolecules*, 2009, **42**, 6023–6030.
30 N. Du, G. P. Robertson, J. Song, I. Pinnau, S. Thomas and M. D. Guiver, *Macromolecules*, 2008, **41**, 9656–9662.
31 N. Du, G. P. Robertson, I. Pinnau, S. Thomas and M. D. Guiver, *Macromol. Rapid Commun.*, 2009, **30**, 584–588.
32 W. M. Lee, *Polym. Eng. Sci.*, 1980, **20**, 65–69.
33 A. Bondi, *J. Phys. Chem.*, 1964, **68**, 441–451.
34 H.-l. Lv, B.-G. Wang and Y. Kong, *Polym. J.*, 2009, **41**, 1049–1054.
35 Y. H. Zhao, M. H. Abraham and A. M. Zissimos, *J. Org. Chem.*, 2003, **68**, 7368–7373.
36 C. E. Sroog, *Prog. Polym. Sci.*, 1991, **16**, 561–694.
37 J. Ishii, A. Takata, Y. Oami, R. Yokota, L. Vladimirov and M. Hasegawa, *Eur. Polym. J.*, 2010, **46**, 681–693.